Atomistic simulation of CdTe solid-liquid coexistence equilibria

Chuck Henager, Jr.[1,*] and James R. Morris[2]
[1]*Pacific Northwest Laboratory, Richland, Washington 99352, USA*
[2]*Oak Ridge National Laboratory, Oak Ridge, Tennessee 37830, USA*
(Received 1 July 2009; revised manuscript received 7 October 2009; published 7 December 2009)

Atomistic simulations of CdTe using a Stillinger-Weber (SW) interatomic potential were undertaken to model the solid-liquid phase equilibria of this important compound semiconductor. Although this potential has been used by others to study liquid CdTe and vapor-liquid interface, it is based on fitting parameters optimized only for the zincblende solid. It has not been fully explored as a potential for solid-liquid phase equilibria until this work. This research reports an accurate determination of the melting temperature, $T_M=1305$ K near $P=0$, the heat of fusion at melting, and on the relative phase densities with a particular emphasis on the melting line. The SW potential for CdTe predicts a liquid with a density slightly less than that of the solid and, hence, the pressure-temperature melting line has a positive slope. The pair-correlation structure of the liquid is determined and favorably compared to neutron-scattering data and to *ab initio* simulations. The liquid-solid interface is discussed using density profiles and a short-range order parameter for models having principal orientations along ⟨100⟩, ⟨110⟩, and ⟨111⟩ crystallographic directions.

DOI: 10.1103/PhysRevB.80.245309 PACS number(s): 81.10.Aj, 02.70.Ns, 61.20.Ja, 64.70.dj

I. INTRODUCTION

Melt-grown compound semiconductors, such as CdZnTe (CZT), for radiation detection applications represent a severe materials challenge when the requirements are for large, defect-free crystals with high resistivity and large electron mobility-lifetime products grown reproducibly and with high growth yields. Depending on the application single-crystal cubes of CZT as large as 20 mm on a side are required. At present this is not possible and one of the reasons includes a lack of fundamental understanding of the crystal growing process at the appropriate length scale having to do with defect formation. For a ternary or binary system there are complexities that appear to be fairly daunting in developing this understanding at an atomic level and one of the principal limitations is the lack of accurate interatomic potentials to facilitate studies such as have been undertaken for unary systems that begin to provide some of the fundamental knowledge that is currently lacking.[1–8] For binary and ternary systems, there are additional complications, as there may be important compositional effects at the interface that are absent in monatomic systems. The use of mesoscale models of crystallization, such as phase field models, requires accurate and detailed information on solid-liquid interface kinetics, anisotropies, and compositional parameters near the interface. Such details can be gleaned from accurate atomistic models of solid-liquid interfaces, as well as additional and critical information for crystal growth.

Inputs required for more accurate models of CZT growth are anisotropic interface energies, attachment kinetics, compositional fluctuations in the liquid, and growth orientation selection. Prior to devoting the time necessary for obtaining these details, a testing and development of improved interatomic potentials for CZT has been undertaken beginning with an investigation of a Stillinger-Weber (SW) potential for CdTe developed for studies of the liquid phase.[9] This potential, however, is not expected to be able to accurately provide all of the required details since it was parameterized using only the zincblende structure for CdTe, which does not provide for Te-Te or Cd-Cd interactions. In particular, the lack of accurate Te-Te interactions will prevent the liquid structure from achieving the same results obtained using *ab initio* methods that revealed the formation of branched Te chains and Cd clusters in liquid CdTe simulations, along with other more fundamental liquid properties.[10–12] Moreover, while this potential has been used to study liquid structures using molecular dynamics (MD), the simulations employed very small periodic models and short simulation times with apparent contradictory results in terms of the quality of the potential and the calculations of liquid structure factors.[13,14]

This work represents the first test of this potential using large-scale MD simulations and a more detailed study of the solid-liquid transition, both in terms of the equilibrium melting line[15] but also examination of the liquid structure and density as a function of distance from the solid-liquid interface and interface crystallographic orientation. In doing so we follow many of the procedures developed for the study of unary systems.[15–26] In particular, this work focuses on stoichiometric CdTe and represents an initial set of studies in this system.

II. COMPUTATIONAL DETAILS

As indicated above, simulations were made using the SW potential for CdTe developed by Wang;[9] the potential energy has the form

$$V=\sum_{i<j} W_2(r_{ij})+\sum_{i<j<k} W_3(\mathbf{r_i},\mathbf{r}_j,\mathbf{r}_k). \quad (1)$$

The two-body term W_2 is zero for distances larger than the cut-off value $r_c=1.8\sigma$, with $\sigma=2.51$ Å. For smaller distances, W_2 has the form

$$W_2(r) = \varepsilon A_{\alpha\beta}[B_{\alpha\beta}(\sigma/r)^4 - 1]\exp[\sigma/(r - r_c)]. \quad (2)$$

In this expression, α designates the element type (Cd or Te) for atom i and β designates the type for atom j. The three-body term W_3 is

$$W_3 = \varepsilon[h(r_{ij}, r_{ik}, \theta_i) + h(r_{ij}, r_{jk}, \theta_j) + h(r_{ik}, r_{jk}, \theta_k)], \quad (3)$$

where θ_i is the angle centered on atom i and its neighbors j and k. Here, the function $h(r,s,\theta)$ is zero if r or s are greater than r_c. Otherwise, it has the form

$$h(r,s,\theta) = \lambda \exp[\nu\sigma(r - r_c)^{-1} + \nu\sigma(s - r_c)^{-1}]\left(\cos\theta - \frac{1}{3}\right)^2. \quad (4)$$

Note that W_3 is independent of the types of atoms i, j, and k. Due to the fact that the angles $\{\theta_i\}$ are all invariant when all distances are scaled by the same factor, the isotropic pressure may be calculated using the same virial expressions as for pair potentials. All parameters for the potential are given in Ref. 9.

Solid-liquid coexistence models were created with the LAMMPS program.[27] A rectangular prism model of CdTe is created with sizes on the order of $60 \times 6 \times 3a_0^3$, where a_0 is the CdTe lattice parameter, containing a liquid central region in equilibrium with a solid region at either end of the fully three-dimensional (3D) periodic model. The specific sizes are dependent on the interface orientation, with the smaller two simulation cell sizes chosen to be commensurate with the periodicity of the crystal interface. The formation of separate solid and liquid regions is facilitated in LAMMPS by virtue of being able to define and separately control the temperature of portions of the model. In this case, a central region is defined and heated to 2000 K by rescaling the atom velocities in that region alone to create a liquid region, following which the entire model is brought to 1310 K and allowed to equilibrate. The temperature rescaling at 2000 K is run under constant atom number, volume, and energy (NVE) conditions with dynamic rescaling for 10 ps while the rescaling back to 1310 K is performed using similar dynamic rescaling for 10 ps. The central region is then brought to zero pressure under constant atom number, pressure, and temperature (NPT) conditions at 1310 K. All MD is performed using a time step of 1 fs and equilibration runs are always performed under NVE conditions. Three model orientations were chosen for this investigation; [100], [110], and [111] crystal orientations were created along the long axis of the prism such that the solid-liquid interface was normal to the given crystal axis.

Separately, a 3D periodic CdTe cube model $10 \times 10 \times 10a_0^3$ was ramped from an initial temperature of 500–1700 K in 1.9 ns, 0.62 K/ps; under moderately slow NPT conditions to achieve an all-liquid model. At 1.9 ns the model began to melt at 1700 K and at 2.3 ns had achieved a temperature of 1307 K in a fully liquid state. This was the first indication of an approximate melting temperature. The model was further heated and reached a final liquid temperature of 1500 K after 2.5 ns. This model was then cooled to 200 K in 1.0 ns, 1.3 K/ps, and remained in noncrystalline state upon cooling. These cube models were used to calculate an approximate melting temperature, solid and liquid densities as a function of temperature, and a heat of fusion for CdTe, required for subsequent calculations.

The coexistence models were created close to thermal equilibrium by bringing the solid and liquid regions to the proper densities by adjusting the dimensions of the rectangular prism to match the calculated solid and liquid densities found in the cube model runs by using NPT thermostatted runs at $T=1310$ K and $P=0$. If this is not done correctly then subsequent approaches to equilibrium are extremely slow. The initial starting two-phase model in the [100] orientation consisted of 0.339 volume fraction liquid in a central region such that the model composite density was consistent with a rule-of-mixtures density for the system. This model was chosen as the starting point for the solid-liquid coexistence runs and it consisted of 8640 atoms in a rectangular prism of $40.12 \times 3.95 \times 1.98$ nm^3 at approximately 1300 K to match the melting temperature determined in the MD runs.

Separate models were created from this initial model by again using NPT runs to adjust both temperature and pressure to new values that ranged in temperature up to 1400 K and in pressure up to 2500 MPa based on the Clausius-Clapeyron equation as

$$\frac{dP}{dT} = \frac{\Delta H_f}{T(V_l - V_s)}, \quad (5)$$

where P is pressure, T is temperature, ΔH_f is the heat of fusion, and V_l and V_s are the liquid and solid specific volumes, respectively, at the melting point of CdTe. The values found in this study were used in Eq. (1) to forecast T-P equilibrium values and these forecasts were used as initial starting points for subsequent NVE runs to allow solid-liquid equilibration under higher model pressures. These methods were repeated uniformly for all models irrespective of their interface orientation. In general, these NVE models were allowed to equilibrate over MD time scales of more than 1 ns.

One method of analyzing the change in structure near the interfaces was by examining a phenomenological order parameter that is large in the solid phase and small in the liquid phase. We use a variation in an order parameter used previously[21] for face-centered cubic (fcc) and body-centered cubic crystals. A set of vectors $\{\boldsymbol{q}\}$ is defined that point along the {110} directions in the crystal portion. There are twelve different directions; taking only one of antiparallel pairs of vectors reduces this to a set of $N_q=6$ vectors. The magnitude of each of these vectors is scaled to be $2\sqrt{2}\pi/a_0$, where a_0 is the cubic-lattice constant. Defined in this way, the *second-nearest*-neighbor vector $\boldsymbol{r}_2$ satisfies $|\boldsymbol{q}_i \cdot \boldsymbol{r}_2| = 0$ or $|\boldsymbol{q}_i \cdot \boldsymbol{r}_2| = 2\pi$. For each atom i, the order parameter is defined as

$$\phi_i = \frac{1}{12N_q}\left|\sum_j \sum_{k=1}^{N_q} \exp(\mathbf{r}_{ij} \cdot \mathbf{q}_k)\right|^2, \quad (6)$$

where j runs over all atoms within a cut-off distance chosen to be slightly larger than the magnitude of $\boldsymbol{r}_2$, and k runs over all N_q vectors. This term is essentially a local scattering magnitude and is taking advantage of the fact that the vectors $\{\boldsymbol{q}\}$

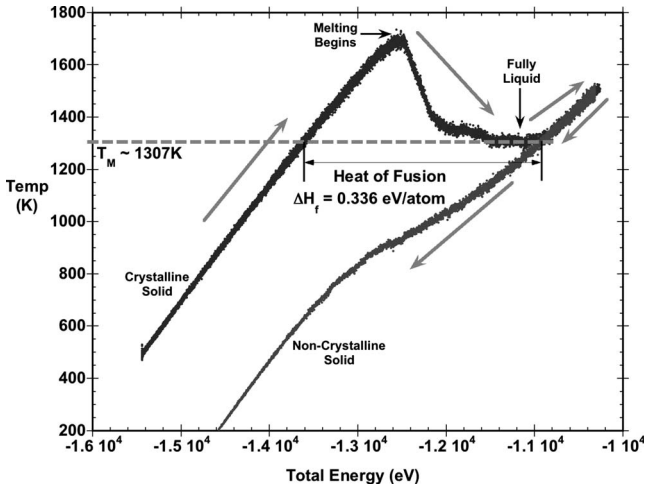

FIG. 1. Model temperature (K) as a function of total energy (eV) for 1000 CdTe unit cells (8000 atoms) as model temperature is ramped from 500 to 1700 K, where it begins to melt and subsequently cools to 1307 K, continuing up to 1500 K and then cooled down to 200 K, where it remains noncrystalline. The approximate melting temperature is indicated along with the heat of fusion for CdTe (eV/atom).

are along equivalent reciprocal lattice directions for the fcc (and diamond) lattice, which forms the basis for the zincblende structure. The factor of 12 is used to account for the 12 second-nearest neighbors.

III. RESULTS AND DISCUSSION

Figure 1 shows the model temperature versus total energy as the CdTe cube model is heated, melted at 1700 K, and then cooled as a liquid into a noncrystalline solid at 200 K. The energy difference between the two models at the approximate melting temperature of 1307 K, one solid and one liquid, gives the heat of fusion for CdTe. These models also provide solid and liquid densities as a function of temperature. The CdTe solid has a density of 5.578 g/cm^3 at 1300 K in our MD models compared to 5.727 g/cm^3 experimentally, while the model liquid density was 5.326 g/cm^3 compared to 5.665 g/cm^3 in experiments.[28] The heat of fusion determined by MD melting was 270.9×10^3 J/kg (15.5 kcal/mol) compared to experimental values of 209.2×10^3 J/kg (12.0 kcal/mol).[9] Wang and Stroud[9] found a similar value of 252.8×10^3 J/kg (14.5 kcal/mol) in their Monte Carlo study using this potential. The approximate melting temperature determined here was ~1307 K, which differs from what Wang and Stroud reported as ~1370 K. The difference can partly be attributed to the accuracy of the coexistence method and partly to increased computational capabilities, including the use of larger atomistic models, due to advances in computer hardware.

The liquid model was analyzed for liquid structure factors using pair-correlation methods and this data is shown in Fig. 2, which compare favorably with the total $g(r)$ from *ab initio* CdTe liquid-model data[11] and from neutron-diffraction data.[29,30] The most significant discrepancy is that *ab initio* models suggest a Cd-Cd nearest-neighbor peak in the liquid

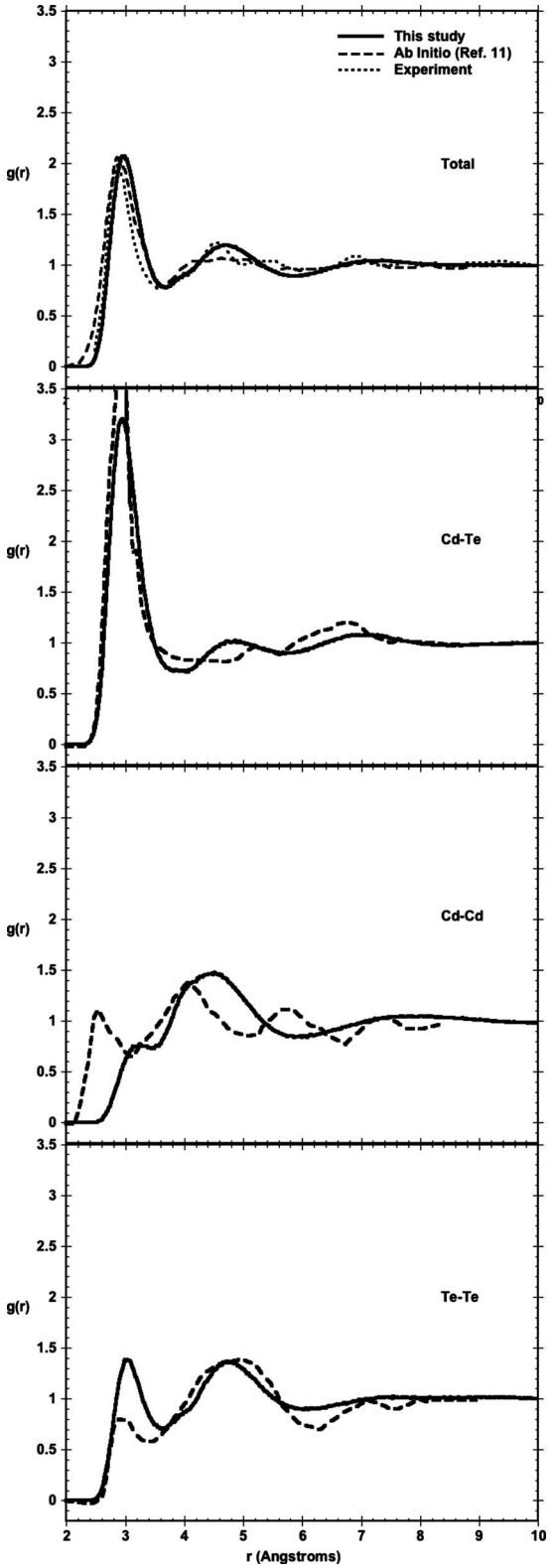

FIG. 2. The total and partial pair-correlation data from liquid models generated in this work at 1305 K, and compared to curves from *ab initio* models (Ref. 11) and to neutron-diffraction data from liquid CdTe (Ref. 29).

that is much shorter than what is seen in the present simulations. These *ab initio* results appear to produce an increased value of $g(r)$ in the range of 2.2–2.4 Å that is not seen in

either our results or in experimental results. In fact, the present simulations appear to reproduce the experimental $g(r)$ curve better than *ab initio* results, though this should be considered somewhat fortuitous, given the limitations of the potential. Earlier MD simulations with the same potential gave pair-correlation data that was not in good agreement with either experiment or with the *ab initio* results.[13] Although the conclusion in that former study was that the SW potential for CdTe was inferior, the present study shows that using larger models and longer simulation times than the former study can generate reasonable agreement with existing data and with *ab initio* results. The reason for this agreement is that liquid CdTe retains a basic tetrahedral coordination for temperatures near melting and for low pressures, which is close to the conditions used for the parameterization of this CdTe SW potential. The tetrahedral behavior of this potential has been noted before.[9] Specifically, we calculate an average coordination slightly higher than four in the liquid state (within a cutoff of 3.6 Å, close to the minimum of the pair-correlation function). This coordination is in agreement with those from *ab initio* simulations (see Ref. 11, Table II). The average angle distribution is peaked close to 100°, slightly less than the value of 109° expected for a perfectly tetrahedral material. Studies of CdTe solid-liquid equilibria near the melting temperature using this potential can be expected to provide useful information because of this agreement even given the limitations of the potential.

While the melting/crystallization results provide a simple estimate of the melting temperature, it is not necessarily accurate. Coexistence simulations provide a more direct approach for accurately determining the melting temperature and results on different interfaces provide a check on the consistency of the results. Coexistence results in terms of temperature-pressure pairs at equilibrium using converged NVE runs are shown in Fig. 3 as the melting line for CdTe with this interatomic potential. The interface orientation is labeled in Fig. 3 and, while there are differences between these MD results as a function of interface orientation the differences are not large. The most important point to be made from the MD data is that the SW potential for CdTe produces a melting line with a positive upwards slope of 0.023 K/MPa, which is comparable to the experimental value given by Glazov[28] of 0.0125 K/MPa. This indicates that the simulated CdTe is not a waterlike or Si-like liquid as suggested by the data of Jayaraman,[31] which gives a melting line that slopes downward at −0.046 K/MPa. The positive slope for the melting line is consistent with the observation that the liquid density for CdTe in the MD models was less than that of the corresponding solid.

The melting temperatures calculated from the different interfaces are reasonably consistent, within 5% of each other. The (111) interface simulations produce a slightly higher melting temperature than the (100) and (110) interfaces; this appears to be due to slightly different lattice parameters in the in-plane direction, suggesting a slightly anisotropic stress contribution. The differences in *P-T* equilibrium between the three orientations appears to have more to do with the equilibration time in the MD runs and should not be interpreted as an intrinsic difference in melting behavior. For similar size models the (111) orientation took approximately twice as

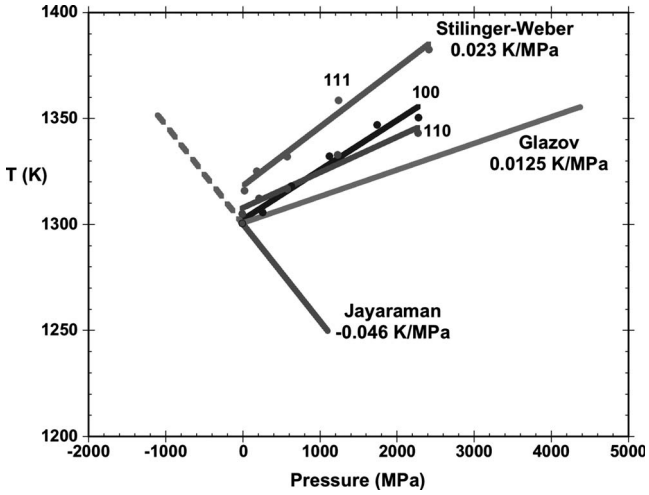

FIG. 3. *P-T* equilibrium curve, or melting line, for CdTe as determined by the NVE MD coexistence runs for atomic models oriented with solid-liquid interface normal to indicated crystallographic orientation. The data are from Jayaraman (Ref. 31) and Glazov (Ref. 28). The MD data indicate that the melting line is independent of interface orientation and that differences in the (111) data are due to model equilibration times (see text).

long to equilibrate as the other two orientations during NVE MD, which suggests that different interface orientations have significantly different kinetic processes linked to solidification and/or melting processes; in particular, it suggests that the (111) interface has a lower interfacial mobility. Since it is likely that interface energies for CdTe are anisotropic and, since it is known that related diamond cubic materials, such as Si and Ge, have transitions between rough and faceted interfaces depending on interface orientation, we investigated the local order and local densities of the three interfaces using the MD data generated during the equilibrated NVE runs.

The interface composition, elemental density, and order parameter are shown in Figs. 4–6 for each of the three interfaces in this study. The fine-scale density[24] and order-parameter[21] plots are convenient tools for the study of solid-liquid interfaces in unary and binary systems. Here we examine fine-scale elemental density data and order-parameter plots as a function of location in solid-liquid coexistence models at equilibrium after long-time NVE MD. The density data is averaged over long simulation times, and therefore results near the interface are undoubtedly affected by fluctuations in the height of the interface. However, the positions of the interfaces do not move much during the simulation, and in the simulations, the periodic box has narrow cross-sections, which limit fluctuations in the height of the interface. The order-parameter calculation is based on the final configuration; we note that the widths estimated from this single configuration are comparable to the widths based on the density profile, indicating that the long time averages do not significantly affect our estimates of the interfacial widths. Figure 4 shows the results for the (100) interface, Fig. 5 for the (110) interface, and Fig. 6 for the (111) interface. While differences are seen in all of the figures, some critical features are observed in the (111) interface plot that

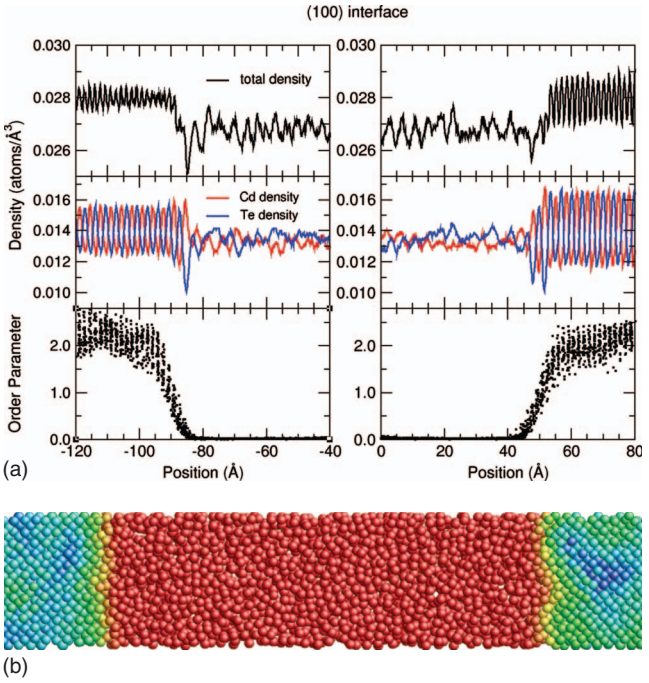

FIG. 4. (Color) Fine-scale density and order-parameter plots as functions of position normal to the interface for (100) CdTe. The upper plot (a) shows total density, the middle plot shows elemental density, and the lower plot shows atomic order parameter. The (100) interface is sharp but CdTe liquid contains remnants of tetrahedral ordering near the interface and for several nanometers into the liquid. The lower figure (b) is a two-dimensional (2D) atom plot color coded to order parameter with blue as ordered and red as disordered or liquid.

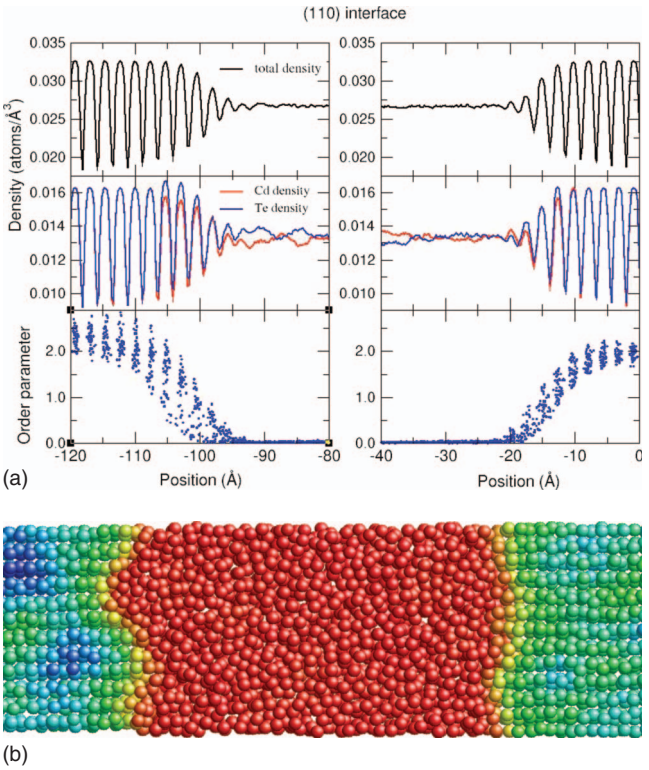

FIG. 5. (Color) Fine-scale density and order-parameter plots as functions of position normal to the interface for (110) CdTe. The upper plot (a) shows total density, the middle plot shows elemental density, and the lower plot shows atomic order parameter. The lower figure (b) is a 2D atom position plot color coded to order parameter as in Fig. 4.

are not seen in the other data. Specifically, the (111) interface is broader, shows structural twins, and shows strong compositional segregation in the liquid.

First, the (100) interface density data show that tendency for the tetrahedral coordination that is parameterized into the SW potential to persist into the liquid for several nanometers. CdTe total-density oscillations are observed up to 40 Å into the liquid (right-hand side of Fig. 4). The individual Cd and Te densities appear to oscillate out of phase in the liquid near the interface, likely induced by the similar out of phase chemical oscillations of the (100) planes in the crystal phase. This demonstrates that chemical ordering due to the interface can persist for significant depths into the liquid phase. The solid-liquid interface is about 15 Å in width, as defined by the distance to go from fully ordered to fully disordered. The melting point for this model was determined to be 1305 K from the NVE MD data. The (110) interface width is also about 15–20 Å as shown in Fig. 5, but the liquid composition profiles are less structured than the (100) liquid and fewer density oscillations are observed near the interface. The absence of chemical ordering in the liquid near the interface is not surprising as the (110) crystal planes contain both Cd and Te atoms, unlike the (100) crystal planes.

In contrast, the (111) interface, which is a polar interface, demonstrates a critical feature for CdTe as the (111) stacking order for the zincblende structure of aAbBcC gives one interface Cd terminated and the other interface Te terminated in the coexistence model. Periodic boundary conditions forces there to be two different solid-liquid interfaces in our model, and for this geometry the two interfaces must be terminated by different species. This can be seen clearly in Fig. 6 plots of elemental densities. The Cd-terminated interface on the left-hand side of Fig. 6 reveals that there is a Te-rich region in the liquid at that interface, while there is a corresponding Cd-rich liquid region adjacent to the Te-terminated interface on the right-hand side of Fig. 6. In addition, the interface width is now seen to be about 15–20 Å, as determined by the density profile. The atom model shows the facets and some twins near the solid-liquid interface. This affects the width of the order-parameter profile, as the twinned region has a lower order parameter due to the differences from ideal stacking. Figure 7 shows a ball and stick model of the CdTe (111) interface with a (111) twin identified as a coherent boundary parallel to the (111) plane with stacking sequence of CcAaBbC|cBbAaCc.[32,33] This structure naturally occurs during the simulations. Such lamellar twins have low energies, 0.016 J/m^2, as determined from *ab initio* models. Since the SW potential used in the present simulations only contains nearest-neighbor interactions, the lamellar twin energy is exactly zero. Steps or facets along the (111) solid-liquid interface are also seen in the atomic model. Note that electrostatic effects due to ionic charges at polar interfaces are not included in our model; we assume that electronic charge transfer will screen out any long-ranged

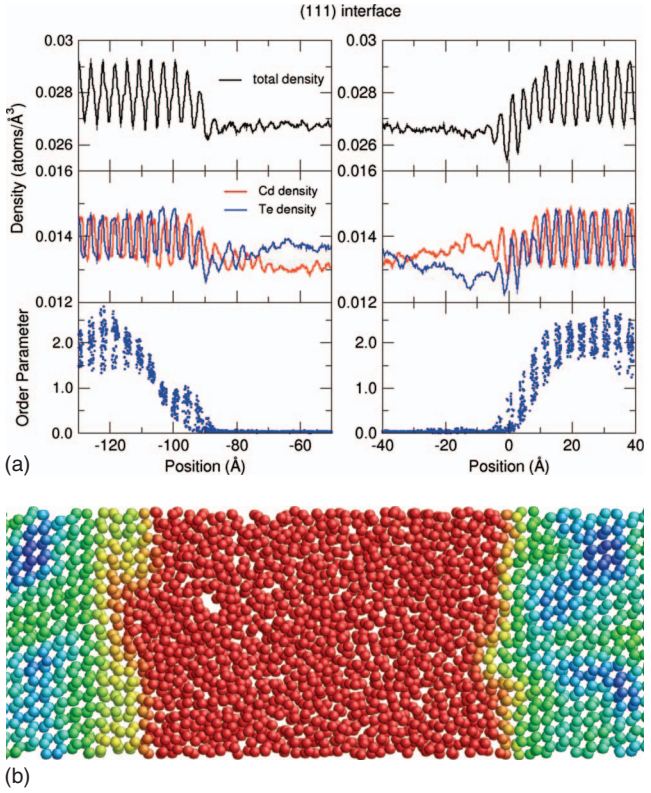

FIG. 6. (Color) Fine-scale density and order-parameter plots as functions of position normal to the interface for (110) CdTe. The upper plot (a) shows total density, the middle plot shows elemental density, and the lower plot shows atomic order parameter. The CdTe liquid contains significant compositional segregation near the interfaces and also contains (111) lamellar twins (see text and Fig. 7). The lower plot (b) is a 2D atom position plot color coded to order parameter as in Figs. 4 and 5.

polarization fields, even though electronic degrees of freedom are of course not explicitly included in classical simulations of this type.

Experimentally, the growth of CdTe from the melt is observed to involve twinning, thought to be mechanical twinning due to thermal strains, and it is interesting to see twins form spontaneously in these atomic models where the thermal strains are likely not the root cause. Rather, the low values for CdTe stacking fault energies and twin boundaries[32] almost ensures that such defects will be present during crystal growth. Of more concern for devices, however, is the presence of Te particles that form during melt growth of CdTe and CZT. These observations of the elemental segregation in the liquid may be a partial explanation for the formation of Te-rich inclusions during solidification.[34–36] One hypothesis for Te-particle formation during crystallization has been the incorporation of liquid-Te droplets into the growing crystal in contrast to subsequent precipitation of Te during solidification and cool down due to nonstoichiometry in the crystal. The development of Te-rich liquid regions adjacent to solid-liquid interfaces has not been considered but would offer a partial explanation for the relatively easy formation of such Te particles. Also, the chemical segregation near the interface may interfere with planar growth, causing growth instabilities similar to those observed in alloys. Our observation of chemical segregation near the interface in a congruently melting system is significant, and undoubtedly plays an important role in crystal growth.

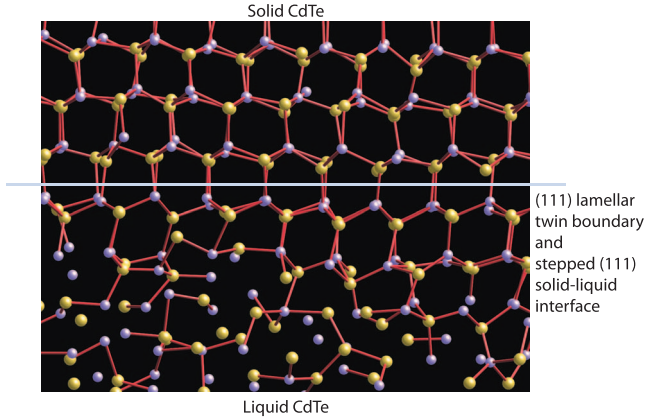

FIG. 7. (Color) A ball and stick model of a portion of CdTe solid-liquid interface for the (111) orientation shown in Fig. 6 is shown. A (111) lamellar twin is indicated in the figure and steps are observed along the solid-liquid interface.

A number of further calculations are underway. First, the compositional segregation near the (111) interfaces is of particular interest to the growth of single-crystal CdTe, and the results presented here suggest that this compositional segregation may extend much further than may be explored using the present simulations. Larger simulations of this interface are currently being performed, and a more detailed analysis of the structure will be examined and compared to ordering in liquid Si as examined using a similar Stillinger-Weber potential.[6] It is also interesting to note that CdTe is a line compound experimentally; similarly, in our simulations the crystal remains highly ordered and stoichiometric. It is of interest to explore not only the pressure-temperature behavior of the phase diagram but also the composition-temperature behavior. This is more challenging when the simulated system as a whole is not stoichiometric, due to the fact that as the crystal grows or melt (to achieve equilibrium), the liquid changes composition with the composition near the interface changing most rapidly. True equilibrium therefore requires compositional diffusion through the liquid, which necessarily requires much longer simulations and longer statistics. An alternative approach would be to use semigrand canonical Monte Carlo simulations, as has been applied to other alloy systems.[37]

Also of interest are the growth mode and interfacial mobilities of the different planes. The growth of the facetted (111) interface for Stillinger-Weber Si has been examined from the point of view of step motion on this plane.[5] This will be of particular interest to examine for CdTe, due to the fact that growth of planes (or step motion) may be similar, except that the growth will likely be much slower due to the chemical ordering that occurs as the crystal grows. This is particularly true given the compositional changes near the interface, as shown in Fig. 6. Again, there are two distinct (111) interfaces (one Cd terminated, one Te terminated), and they may exhibit different behaviors.

Finally, this work is based on a rather simple potential, and a number of aspects of this potential are either limited or

require further testing. One significant issue is that the potential is very short ranged, essentially a nearest-neighbor model. This unphysical short-range cutoff results in a twin energy that is identically zero: within the range of the potential, the different stacking sequence does not alter the neighbor configurations. Thus, twins will be more likely to form than in the real system. However, as twinning is prevalent in the real system, due to the low energy of the twins, it is not apparent how much this affects the results. Second, the II-VI semiconductors have both covalent and ionic contributions to the bonding. The present potential mimics some of this by strongly favoring Cd-Te bonds over Cd-Cd and Te-Te bonds, but again does this in a purely local approach. The ionic contribution is longer ranged, and therefore is likely to play a role both in the twin energy and in determining structure and composition near the solid-liquid interface. All of these issues should be explored further, with a goal of developing more accurate potentials that incorporate these effects in a physical manner.

IV. CONCLUSIONS

Atomistic simulations of solid-liquid coexistence models in the CdTe system using a Stillinger-Weber potential have provided details of the CdTe melting line and melting temperature. The melting temperature agrees quite well with experimental data at low pressures and the Stillinger-Weber potential successfully enforces the observed tetrahedral coordination of the liquid at ambient pressures that is a known feature of the CdTe low-pressure liquid phase. The melting temperature was found to be 1305 K as compared to 1365 K from experiments[31] and 1370 K from earlier Monte Carlo studies using the same potential.[9] The solid-liquid coexistence approach is considered to be more accurate in this regard. The melting line is in good agreement with experimental results from Glazov,[28] with a positive slope, but the measurements of Jayaraman[31] show a negative slope. Both experiments and our present calculations show a small dependence of the melting temperature on pressure, indicating that the liquid and solid phases are nearly equal in density. In addition, and in contrast to earlier MD simulations, this potential gives reasonable agreement with published neutron-diffraction data and *ab initio* simulations for CdTe liquid pair correlation. The CdTe liquid retains tetrahedral coordination near the interfaces.

Structural and chemical data obtained from careful analysis of compositional density, and order-parameter studies for (100), (110), and (111) solid-liquid interfaces suggests that the (110) interfaces are approximately 10 Å in extent. Significant fluctuations in the (110) interface profile suggest that this interface is "rough," with fluctuations that grow with the area of the interface. Further study of this and the (100) interface is required to determine whether they are truly a rough interface. In contrast, the (111) interface is faceted and can easily form twins. The faceting of this interface is not surprising, given the strong faceting seen in simulations of the Si Stillinger-Weber potential.[5,6,38,39] The (111) interface exhibits strong compositional segregation at least 25 Å into the liquid phase. This compositional segregation near the (111) interfaces may be the cause for the slow equilibration for this orientation, and could also play a role in inhibiting high quality single-crystal growth in these materials.

ACKNOWLEDGMENTS

PNNL is operated for the U.S. Department of Energy by Battelle Memorial Institute under Contract No. DE-AC06-76RLO 1830. This work was funded at PNNL by the Office of Defense Nuclear Nonproliferation, Office of Nonproliferation Research and Development (NA-22). At ORNL this research has been sponsored by the Division of Materials Sciences and Engineering, Office of Basic Energy Sciences, U.S. Department of Energy under Contract No. DE-AC05-00OR-22725 with UT-Battelle.

*Corresponding author. FAX: +1 509 376 0418; chuck.henager@pnl.gov

[1] D. Y. Sun, M. I. Mendelev, C. A. Becker, K. Kudin, T. Haxhimali, M. Asta, J. J. Hoyt, A. Karma, and D. J. Srolovitz, Phys. Rev. B **73**, 024116 (2006).
[2] K. A. Wu, A. Karma, J. J. Hoyt, and M. Asta, Phys. Rev. B **73**, 094101 (2006).
[3] M. Asta, J. J. Hoyt, and A. Karma, Phys. Rev. B **66**, 100101(R) (2002).
[4] J. J. Hoyt, M. Asta, and A. Karma, Phys. Rev. Lett. **86**, 5530 (2001).
[5] D. Buta, M. Asta, and J. J. Hoyt, Phys. Rev. E **78**, 031605 (2008).
[6] D. Buta, M. Asta, and J. J. Hoyt, J. Chem. Phys. **127**, 074703 (2007).
[7] C. A. Becker, D. Olmsted, M. Asta, J. J. Hoyt, and S. M. Foiles, Phys. Rev. Lett. **98**, 125701 (2007).
[8] C. A. Becker, J. J. Hoyt, D. Buta, and M. Asta, Phys. Rev. E **75**, 061610 (2007).
[9] Z. Q. Wang, D. Stroud, and A. J. Markworth, Phys. Rev. B **40**, 3129 (1989).
[10] E. Ko, M. M. G. Alemany, J. J. Derby, and J. R. Chelikowsky, J. Chem. Phys. **123**, 084508 (2005).
[11] V. V. Godlevsky, M. Jain, J. J. Derby, and J. R. Chelikowsky, Phys. Rev. B **60**, 8640 (1999).
[12] V. V. Godlevsky, J. J. Derby, and J. R. Chelikowsky, Phys. Rev. Lett. **81**, 4959 (1998).
[13] V. M. Glazov and L. M. Pavlova, Scand. J. Metall. **31**, 52 (2002).
[14] V. M. Glazov and L. M. Pavlova, J. Cryst. Growth **184-185**, 1253 (1998).
[15] J. R. Morris and X. Song, J. Chem. Phys. **116**, 9352 (2002).
[16] R. L. Davidchack, J. R. Morris, and B. B. Laird, J. Chem. Phys. **125**, 094710 (2006).
[17] B. B. Laird and R. L. Davidchack, J. Phys. Chem. B **109**, 17802 (2005).

[18] R. L. Davidchack and B. B. Laird, Phys. Rev. Lett. **94**, 086102 (2005).
[19] S. Yoo, X. C. Zeng, and J. R. Morris, J. Chem. Phys. **120**, 1654 (2004).
[20] J. R. Morris, Z. Y. Lu, Y. Ye, and K. M. Ho, Interface Sci. **10**, 143 (2002).
[21] J. R. Morris, Phys. Rev. B **66**, 144104 (2002).
[22] R. L. Davidchack and B. B. Laird, Phys. Rev. Lett. **85**, 4751 (2000).
[23] R. L. Davidchack and B. B. Laird, Mol. Phys. **97**, 833 (1999).
[24] R. L. Davidchack and B. B. Laird, J. Chem. Phys. **108**, 9452 (1998).
[25] R. L. Davidchack and B. B. Laird, Phys. Rev. E **54**, R5905 (1996).
[26] J. R. Morris, C. Z. Wang, K. M. Ho, and C. T. Chan, Phys. Rev. B **49**, 3109 (1994).
[27] S. Plimpton, J. Comput. Phys. **117**, 1 (1995).
[28] V. M. Glazov and L. M. Pavlova, High Temp. **39**, 68 (2001).
[29] G. Prigent, R. Bellissent, R. Ceolin, H. E. Fischer, and J. P. Gaspard, J. Non-Cryst. Solids **250-252**, 297 (1999).
[30] J. P. Gaspard, J. Y. Raty, R. Ceolin, and R. Bellissent, J. Non-Cryst. Solids **205-207**, 75 (1996).
[31] A. Jayaraman, W. Klement, and G. C. Kennedy, Phys. Rev. **130**, 2277 (1963).
[32] Y. Yan, M. M. Al-Jassim, and T. Demuth, J. Appl. Phys. **90**, 3952 (2001).
[33] Y. Yan, M. M. Al-Jassim, and K. M. Jones, Thin Solid Films **389**, 75 (2001).
[34] P. Rudolph, Cryst. Res. Technol. **38**, 542 (2003).
[35] P. Rudolph, A. Engel, I. Schentke, and A. Grochocki, J. Cryst. Growth **147**, 297 (1995).
[36] P. Rudolph, Prog. Cryst. Growth Charact. Mater. **29**, 275 (1994).
[37] C. A. Becker, M. Asta, J. J. Hoyt, and S. M. Foiles, J. Chem. Phys. **124**, 164708 (2006).
[38] W. D. Luedtke, U. Landman, M. W. Ribarsky, R. N. Barnett, and C. L. Cleveland, Phys. Rev. B **37**, 4647 (1988).
[39] U. Landman, W. D. Luedtke, M. W. Ribarsky, R. N. Barnett, and C. L. Cleveland, Phys. Rev. B **37**, 4637 (1988).